Synthesis of a New Layered Sodium Copper(II) Pyrophosphate, $Na_2CuP_2O_7$, via an Eutectic Halide Flux

Kristen M. S. Etheredge and Shiou-Jyh Hwu*

Department of Chemistry, Rice University, P.O. Box 1892, Houston, Texas 77251

Received October 28, 1994[⊗]

Crystals of $Na_2CuP_2O_7$ have been grown in a low-temperature eutectic flux of 23% NaCl and 77% CuCl (mp = 315 °C). The X-ray structural analysis shows that this sodium copper(II) pyrophosphate crystallizes in a monoclinic lattice with $a = 14.715(1)$ Å, $b = 5.704(2)$ Å, $c = 8.066(1)$ Å, $\beta = 115.14(1)°$, and $V = 612.9(2)$ Å^3; $C2/c$ (No. 15); $Z = 4$. The structure has been refined by the least-squares method to $R = 0.020$, $R_w = 0.034$, and GOF = 1.93. The framework of the title compound can be described as slabs of $[CuP_2O_7]$, which are composed of undulating $[CuP_2O_7]_\infty$ ribbons, cross-linked by Na cations. The Cu^{2+} cation adopts a CuO_4 square planar coordination geometry which shares four corner oxygens with two P_2O_7 pyrophosphate (diphosphate) groups in a trans orientation and the Na^+ cation appears in a distorted NaO_6 octahedral coordination geometry. The extended $[CuP_2O_7]_\infty$ ribbon structure is constructed by alternating CuO_4 and P_2O_7 units and is characterized by Cu−O−P−O−Cu linkages. In this paper, the synthesis, structure, bonding, thermal property, and infrared spectrum of the title compound are presented. Structural comparison with the $Li_2CuP_2O_7$ and $Sr_2CuSi_2O_7$ phases allows a possible conclusion concerning the role of the A-site cation in the framework formation to be drawn. The relative A−O bond strength and its relationship to the thermal stability, with respect to melting, of the $A_2CuP_2O_7$ (A = Li, Na, K) compound family are illustrated; the unknown structure of the tetragonal $K_2CuP_2O_7$ phase is briefly discussed.

Introduction

Investigation of transition metal silicates and phosphates in A−M−X−O quaternary systems, where A = an electropositive cation, M = a transition metal cation, and X = P or Si, has revealed a large collection of structural families with little correlation to structural types adopted by other transition metal oxide compounds. This is attributed to the unique bonding nature of the tetrahedrally coordinated silicon and phosphorus with oxygens forming oxy anions, e.g., XO_4^{n-} and $X_2O_7^{m-}$ (X = Si^{4+}, P^{5+}; $n = 4, 3$; $m = 6, 4$, respectively). The bonding of these anions can be considered "omnidirectional"; in contrast to the monatomic oxide anions, silicates and phosphates are polyanions whose terminal oxygens are available for bonding with transition metal cations in a variety of ways to form a large class of structurally complex compounds.[1−7] In a manner similar to chalcogenides and halides, the bulky silicate and phosphate oxy anions are polarizable in the sense that the X−O bond interactions are flexible; this may facilitate the formation of a layered framework. In recent studies, a new family of oxosilicate compounds has demonstrated a novel feature where thin two-dimensional transition metal oxide structures are intergrown with the silicate lattice as a backbone, *e.g.*, $[(RE)_4M(Si_2O_7)_2](MO_2)_{4m}$ series (RE = La, Nd, M = Ti and RE = La, M = V for $m = 1$; RE = La, M = Ti for $m = 2$).[4,5]

To study the structure and bonding of analogous oxo compounds associated with late transition metal cations, we have extended our search into the copper-based silicate and phosphate systems. A large collection of ternary and quaternary copper(II) silicates and phosphates are known and many of these structures are complex due to the distorted coordination geometries adopted by CuO_n ($n = 4, 5, 6$).[6,7] Compounds demonstrating layered-like structures are α-$Cu_2P_2O_7$,[6a] β-$Cu_2P_2O_7$,[6b] $Cu_5(PO_4)_2(OH)_4$,[6c,d] and $Li_2CuP_2O_7$.[6e] These reported phases have been prepared by either conventional high-temperature, solid-state precursor methods or hydrothermal techniques. Altered synthetic methods, *e.g.*, changing temperature, reaction mechanism, and basicity/acidity, have led to new discoveries due to these changes in reaction conditions. The title compound, $Na_2CuP_2O_7$, has been isolated via a low-temperature eutectic halide flux. It is a member of the $A_2CuP_2O_7$ (A = Li, Na, K) family, in which only the lithium phase has been structurally characterized thus far. In this paper, the synthesis, structure, bonding, thermal property, and infrared spectrum of the title compound, and a structural comparison with the $Li_2CuP_2O_7$[6e]

[⊗] Abstract published in *Advance ACS Abstracts,* February 15, 1995.

(1) See, for example: (a) Soghomonian, V.; Chen, Q.; Haushalter, R. C.; Zubieta, J. *Chem. Mater.* **1993**, *5*, 1595. (b) Soghomonian, V.; Chen, Q.; Haushalter, R. C.; Zubieta, J.; O'Connor C. J.; Lee, Y.-S. *Chem. Mater.* **1993**, *5*, 1690.

(2) (a) Wang, S.; Hwu, S.-J. *J. Solid State Chem.* **1991**, *90*, 31. (b) Hwu, S.-J.; Willis, E. D. *J. Solid State Chem.* **1991**, *93*, 69.

(3) (a) Serra, D. L.; Hwu, S.-J. *J. Solid State Chem.* **1992**, *101*, 32. (b) Serra, D. L., Ph.D. Dissertation, Rice University, 1994.

(4) (a) Wang, S., Ph.D. Dissertation, Rice University, 1993. (b) Wang, S.; Hwu, S.-J. *J. Am. Chem. Soc.* **1992**, *114*, 6920. (c) Chen, S. C.; Ramanujachary, K. V.; Greenblatt, M. *Inorg. Chem.* **1994**, *33*, 5994.

(5) (a) Wang, S; Hwu, S.-J. *Inorg. Chem.* **1995**, *34*, 166. (b) Wang, S.; Hwu, S.-J.; Paradis, J. A.; Whangbo, M.-H. *J. Am. Chem. Soc.*, submitted for publication.

(6) (a) Robertson, B. E.; Calvo, C. *Acta Crystallogr.* **1967**, *22*, 665. (b) Robertson, B. E.; Calvo, C. *Can. J. Chem.* **1968**, *46*, 605. (c) Shoemaker, G. L.; Kostiner, E. *Am. Mineral.* **1981**, *66*, 176. (d) Shoemaker, G. L.; Anderson, J. B.; Kostiner, E. *Am. Mineral.* **1981**, *66*, 169. (e) Spirlet, M. R.; Rebizant, J.; Liegeois-Duyckaerts, M. *Acta. Crystallogr.* **1993**, *C49*, 209.

(7) (a) Shoemaker, G. L.; Anderson, J. B.; Kostiner, E. *Acta Crystallogr.* **1977**, *B33*, 2969. (b) Anderson, J. B.; Shoemaker, G. L.; Kostiner, E. *J. Solid State Chem.* **1978**, *25*, 49. (c) Brunel-Laügt, M.; Durif, A.; Guitel, J. C. *J. Solid State Chem.* **1978**, *25*, 39. (d) Brunel-Laüt, M.; Guitel, J. C. *Acta Crystallogr.* **1977**, *B33*, 3465. (e) Kawamura, K.; Kawahara, A.; Iiyama, J. T. *Acta Crystallogr.* **B34**, 3181 (1978). (f) Kawamura, K.; Kawahara, A. *Acta. Crystallogr.* **1976**, *B32*, 2419. (g) Senga, Y.; Kawahara; A. *Acta Crystallogr.* **1980**, *B36*, 2555. (h) Martin Pozas, J. M.; Rossi, G.; Tazzoli, V. *Am. Mineral.* **1975**, *60*, 471. (i) Shoemaker, G. L.; Kostiner, E.; Anderson, J. B. *Z. Kristallogr.* **1980**, *152*, 317. (j) Effenberger, H. *Z. Kristallogr.* **1987**, *180*, 43. (k) Anderson, J. B.; Kostiner, E.; Ruszala, F. A. *J. Solid State Chem.* **1981**, *39*, 29. (l) Pabst, A. *Acta Crystallogr.* **1959**, *12*, 733. (m) Ito, J.; Peiser S. *J. Res. Natl. Bur. Stand.* **1969**, *73A*, 69.

0020-1669/95/1334-1495$09.00/0 © 1995 American Chemical Society

Table 1. Crystallographic Data[a] for $Na_2CuP_2O_7$

chem formula	$Na_2CuP_2O_7$	fw	283.47
a, Å	14.715(1)	space group	$C2/c$ (No.15)
b, Å	5.704(2)	T, °C	23
c, Å	8.066(1)	λ, Å	0.710 69
β, deg	115.14 (1)	ϱ_{calcd}, g cm^{-3}	3.073
V, Å^3	612.9(2)	linear abs coeff, cm^{-1}	149.19
Z	4		
R[b]	0.020		
R_w[c]	0.034		

[a] The cell constants are refined in the monoclinic crystal system by using 25 high angle reflections ($30.93° \leq 2\theta \leq 39.73°$). [b] $R = \sum[|F_o| - |F_c|]/\sum|F_o|$. [c] $R_w = [\sum w[|F_o| - |F_c|]^2/\sum w|F_o|^2]^{1/2}$.

and $Sr_2CuSi_2O_7$[7m] phases are presented. The unknown structure of the tetragonal $K_2CuP_2O_7$[8] phase is briefly discussed.

Experimental Section

Synthesis. Single crystals of $Na_2CuP_2O_7$ were grown by a two-step process. Initially, the $Na_2Cu(PO_3)_4$[9] precursor was prepared by calcining a stoichiometric mixture of $(NH_4)_2HPO_4$ (Fisher, 99.4%), CuO (Strem, 99.999%), and Na_2CO_3 (Mallinckrodt, 99.9%) in air at 325 °C. Next, a stoichiometric amount of Cu_2O (Aldrich, 97%) was added to the sodium copper phosphate precursor preparing a reaction mixture with nominal composition $Na_2Cu_5(P_2O_7)_2$. An eutectic flux of 23% NaCl (EM Science, 99.9%) and 77% CuCl (Aldrich, 99+%), mp = 315 °C,[10] was employed with a flux to charge ratio of 5:1 for the crystal growth experiment. The mixture was placed in an evacuated, carbon-coated silica ampule and heated at 500 °C for 8 days and then cooled at 3 °C/h to room temperature. Blue, plate crystals of the title compound (30% yield) were isolated by washing the reaction product with deionized water using a suction filtration method. The rest of the reaction products were in powder form and were unidentifiable except for the insoluble CuCl. Bulk quantity $Na_2CuP_2O_7$ was prepared from a direct reaction of stoichiometric mixture of NaH_2PO_4 (Aldrich, 99.9%) and CuO at 525 °C for 5 days. The final reaction product was a pure phase based upon powder X-ray diffraction analysis.

The analogous compounds, $Li_2CuP_2O_7$ and $K_2CuP_2O_7$, were also prepared in a polycrystalline form for the infrared spectroscopy and ion-exchange studies described below. The $Li_2CuP_2O_7$ phase can be synthesized in a manner similar to that mentioned above from a mixture of LiH_2PO_4 (Aesar, 97%) and CuO with slow heating to the maximum temperature of 615 °C, where the reaction mixture was heated for 2 days. The $K_2CuP_2O_7$ powder was prepared by a two-step reaction procedure. A mole of K_2CuO_2 precursor, calcined from a stoichiometric mixture of K_2CO_3 (Mallinckrodt, 99%) and CuO at 850 °C, was reacted with 2 mol of $(NH_4)_2HPO_4$ at 575 °C for the approximately same length of time as its lithium analog. The final products were all subject to the powder X-ray diffraction examination which showed them to be pure phases.

Structure Determination. A light blue, plate crystal was mounted on a glass fiber for single-crystal X-ray diffraction study. The diffraction data were collected at room temperature on a Rigaku AFC5S four-circle diffractometer. Crystallographic data for the title compound are summarized in Table 1. The unit cell parameters and the orientation matrix for data collection were determined by a least-squares fit of 25 peak maxima with $7° < 2\theta < 30°$. There was no detectable decay during data collection, according to the intensities of three standard reflections (1,−1,−1; −1,−1,0; −1,−1,−1) which were measured every 150 reflections. The TEXSAN software package[11] was used for crystal structure solution and refinement. Data reduction, intensity analysis, and extinction conditions were determined with the program PROCESS. Lorentz−polarization and empirical absorption corrections based on three computer chosen azimuthal scans (2θ = 24.63, 30.92, 32.88°) were applied to the intensity data. On the basis of extinction conditions and correct structure solution, space group $C2/c$ (No. 15) was chosen. The atomic coordinates of Na, Cu, and P were determined using the SHELXS-86 program,[12] and those of oxygen atoms were resolved by using a Difference Fourier map. The structural and thermal parameters were refined by the full-matrix least-squares method to $R = 0.020$, $R_w = 0.034$, and GOF = 1.93. Table 2 lists the final positional and thermal parameters.

Table 2. Positional and Isotropic Thermal Parameters[a] for $Na_2CuP_2O_7$

atom	x	y	z	B_{eq}, Å^2
Cu	0	0	0	0.90(2)
P	0.39521(4)	0.15897(9)	0.15585(6)	0.66(2)
Na	0.22924(7)	0.1402(1)	0.2991(1)	1.20(3)
O(1)	1/2	0.0181(3)	1/4	0.84(8)
O(2)	0.1877(1)	0.4839(2)	0.3982(2)	1.02(5)
O(3)	0.3930(1)	0.3324(3)	0.2992(2)	1.28(5)
O(4)	0.1020(1)	0.2129(3)	0.0077(2)	1.27(5)

[a] Equivalent isotropic thermal parameters defined as $B_{eq} = (8\pi^2/3)$ trace U.

Thermal Analysis. Differential thermal analysis (DTA) was performed on a DuPont 9900 thermal analysis system. The analysis was carried out by using ground single crystals as well as the polycrystalline samples prepared above. The analysis was performed from 25 to 675 °C for K/Na and 800 °C for Li with a heating rate of 10 °C/min. A fused quartz ampule was used for containing polycrystalline samples. The Al_2O_3 powder was employed for the sealed reference tube. The results showed that the melting point of the title compound is as low as 643.1 °C, much lower than that of early transition metal phosphates. The melting points for the Li and K powder samples are at 775.8 and 476.2 °C, respectively.

Infrared Spectroscopy. The infrared (IR) absorption spectra of the $A^I_2CuP_2O_7$ (A = Li, Na, K) compounds family were studied in the range of 1600−400 cm^{-1} wavenumbers and recorded on the Perkin−Elmer 1600 Series FTIR spectrometer with 16 scans and 2.0 cm^{-1} increments. The samples for this study were from ground single crystals (A = Na) and polycrystalline materials (A = Li and K), that were pressed into discs with KBr. The IR spectra of these three compounds show a great resemblance to each other and are presented in Figure 1. The typical frequency ranges corresponding to symmetric (ν_s) vs asymmetric (ν_{as}) P−O−P vibrational modes of the P_2O_7 group are centered at 765/918 cm^{-1} (A = Li), 771/921 cm^{-1} (Na), and 705/908 cm^{-1} (K), respectively. The O−P−O bending and P−O stretching vibrational frequencies associated with the PO_4 group[13] are shown in multiple bands in the 400−660 and 900−1200 cm^{-1} range, respectively. The IR spectra of the $K_2CuP_2O_7$ compound is comparable with that which was reported previously, *e.g.*, 700−707 and 907−910 cm^{-1}, respectively.[8]

Powder X-ray Diffraction. The polycrystalline samples were analyzed by the powder X-ray diffraction (PXRD) technique. The PXRD patterns were collected at room temperature on a Philips PW 1840 diffractometer with Cu Kα radiation (λ = 1.5418 Å) and a Ni filter. NIST (National Institute of Standards and Technology) silicon powder was used as an internal standard. Samples were ground into fine powder and mounted on the sticky side of Scotch brand tape, which was fixed on the sample holder for data collection. For the $Na_2CuP_2O_7$ phase, a total of 17 reflections were indexed and refined by the least-squares program LATT.[14] The refined cell constants were a =

(8) Gabelica-Robert, M. *C. R. Acad. Sci. Paris* **1981**, *293*, 497.
(9) Laügt, M.; Guitel, J. C.; Durif, A.; Martin, C. *C. R. Acad. Sci. Paris* **1967**, *265*, 741.
(10) Levin, E. M.; Robbins, C. R.; McMurdie, H. F. Phase Diagram for Ceramists; The American Cermic Society, Inc.: Columbus, OH, (1964); Figure 12 45.
(11) (a) TEXSAN: Single Crystal Structure Analysis Software, Version 5.0, Molecular Structure Corp., The Woodlands, TX (1989). (b) Cromer, D. T.; Waber, J. T. Scattering Factors for Non-hydrogen Atoms: In *International Table for X-ray Crystallography;* Kynoch Press: Birmingham, England, 1974; Vol. IV, Table 2.2A, pp 71−98.
(12) Sheldrick, G. M. In *Crystallographic Computing 3*; Sheldrick, G. M.; Krüger, C.; Goddard, R., Eds.; Oxford University Press: London/New York, 1985; pp 175−189.
(13) Nakamoto, K. *Infrared and Raman Spectra of Inorganic and Coordination Compounds*, 4th ed.; John Wiley and Sons, Inc.: New York, 1986.
(14) LATT. Takusagawa, F. Ames Laboratory, Iowa State University, Ames, IA, unpublished research, 1981.

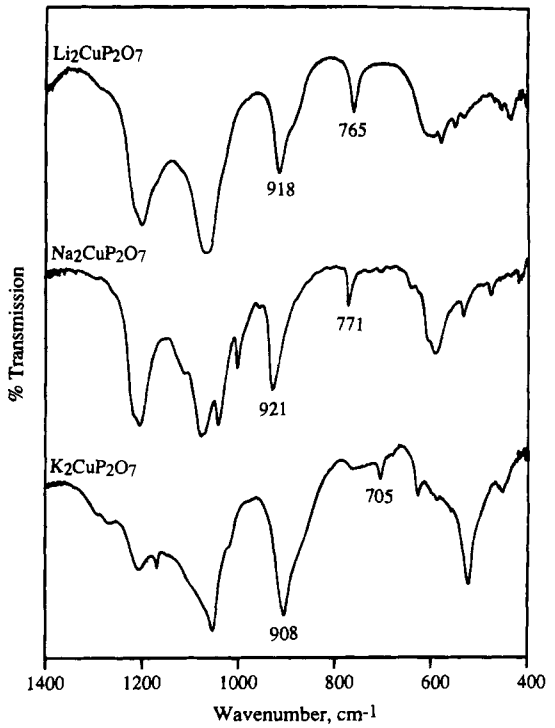

Figure 1. Infrared spectra of (a) $Li_2CuP_2O_7$ (top), (b) $Na_2CuP_2O_7$ (middle), and (c) $K_2CuP_2O_7$ (bottom).

14.718(4) Å, b = 5.702(1) Å, c = 8.063(2) Å, β = 115.04(2)°, which are in good agreement with those determined from single crystal indexing.

Results and Discussion

In this study, choosing an appropriate flux for the crystal growth of the title compound was critical. While the molten halide flux method has proven to be useful for the growth of refractory oxide crystals of early transition metal oxosilicate compounds,[3-5] the halide fluxes used in previous studies, *e.g.*, $BaCl_2$ (mp = 963 °C),[15] are high melting and not suitable for the formation of $Na_2CuP_2O_7$. This is later proven to be because of the low-melting phenomenon of the copper phosphate, which shows a much lower melting point than that of the alkali metal and alkaline-earth metal halides. Thus, an eutectic flux was sought to facilitate a suitable growth window for the crystallization of this low-melting copper phosphate. While the solubility and growth mechanism with respect to the newly employed low-melting flux need to be studied further, crystals of the title compound up to 1.0 × 1.0 × 0.5 mm in size can currently be obtained.

Synthetically, single crystals of $Na_2CuP_2O_7$ can be prepared alternatively through an ion-exchange reaction from polycrystalline $K_2CuP_2O_7$ by employing the NaCl/CuCl flux (mp = 315 °C). This experiment was carried out at 500 °C and the title compound appears to be the only single-crystalline phase found. The PXRD patterns of the complete reaction product show no sign of the presence of the $K_2CuP_2O_7$ phase. Thermodynamically, this suggests that the small A-site cation stabilization drives the ion-exchange process toward the formation of the $Na_2CuP_2O_7$ phase. It is also interesting that the observed melting points for the $A_2CuP_2O_7$ compounds family follow the expected order, $Li_2CuP_2O_7$ (775.8 °C) > $Na_2CuP_2O_7$ (643.1 °C) > $K_2CuP_2O_7$ (476.2 °C), based upon the relative strength of A–O bond, Li–O > Na–O > K–O, according to the pure electrostatic interactions.

(15) *CRC Handbook of Chemistry and Physics*, 71st ed.; Lide, D. R., Ed., 71st ed.; CRC Press, Inc.: Boca Raton, FL, 1990.

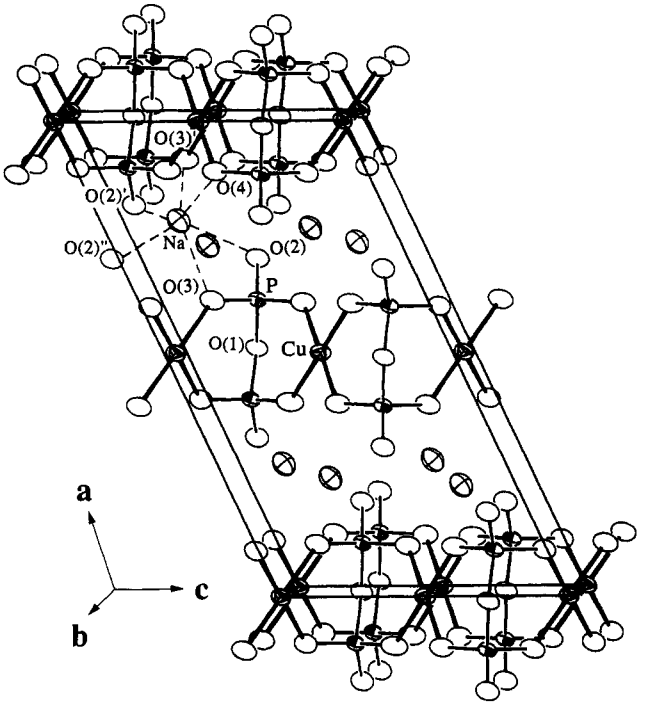

Figure 2. Layered $Na_2CuP_2O_7$ structure shown by the unit cell viewed approximately along the [010] direction. The CuO_4 and P_2O_7 polyhedral coordinations are shown with Cu–O and P–O bonds drawn in thick and thin lines, respectively. The coordination of the NaO_6 polyhedron is presented by dotted lines around one sodium cation for clarity. The anisotropic atoms are presented at 90% probability.

Structurally, the unit cell of the $Na_2CuP_2O_7$ phase adopts an interesting layered framework, as shown in Figure 2. In this figure, the quasi-two-dimensional lattice is characterized by the $[CuP_2O_7]^{2-}$ slabs which are highlighted by thick and thin lines representing the Cu–O and P–O bonds, respectively. The sodium cations, Na^+, reside in the gaps between two copper phosphate slabs with a NaO_6 coordination, as outlined by dotted lines. In the $[CuP_2O_7]^{2-}$ slab, the copper and phosphorus atoms are coordinated to four oxygen atoms each to form square planar and tetrahedral coordination geometries, respectively. Two PO_4 tetrahedra share a common oxygen, O(1), in the P_2O_7 pyrophosphate unit. The CuO_4 and P_2O_7 polyhedra are alternately arranged and connected in a corner-shared fashion. The P_2O_7 unit can be considered as a bidentate ligand chelating the copper cation in a trans orientation, where the bond interactions are characterized by Cu–O–P–O–Cu linkages.

One of the interesting features of the title compound is the undulating $[CuP_2O_7]_\infty$ ribbon. As shown in Figure 3, two $[CuP_2O_7]_\infty$ parallel ribbons are extended along the c axis in a standing wave fashion. This unusual structural arrangement is conceivably attributed to the limitation of tetrahedral bond angle of the P_2O_7 unit that interconnects the CuO_4 units in each ribbon. The two PO_4 groups of the pyrophosphate unit are in a preferred orientation with a nearly eclipsed configuration, as shown in the drawing. The pyrophosphate units are positioned at the peaks of the wave with unshared terminal and bridging oxygen atoms (one terminal oxygen is hidden behind the other) pointing away from the curve. The $[CuP_2O_7]^{2-}$ slab structure is constructed by the $[CuP_2O_7]_\infty$ parallel ribbons stacked "constructively" according to the "phase" of the waves, *i.e.*, the apical oxygen atoms of the P_2O_7 unit are pointing into the valley of the neighboring ribbon. In the partial structure of the extended $[CuP_2O_7]^{2-}$ slab (Figure 3), the two parallel ribbons are cross-linked by the sodium cations. The sodium cations are actually situated above and below the space between the two parallel

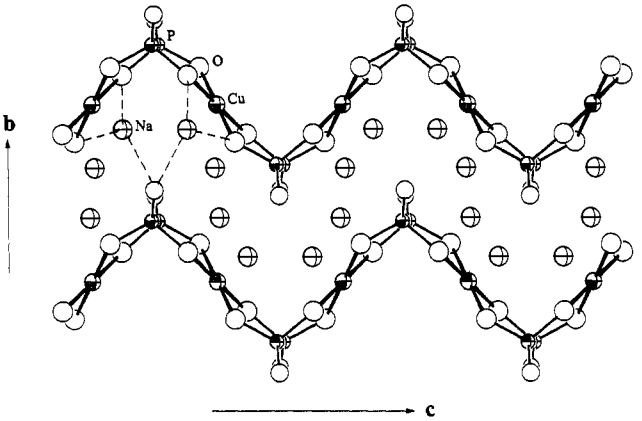

Figure 3. Partial structure of the extended $[CuP_2O_7]^{2-}$ slab shown by two undulating $[CuP_2O_7]_\infty$ ribbons that are cross-linked by the sodium cations.

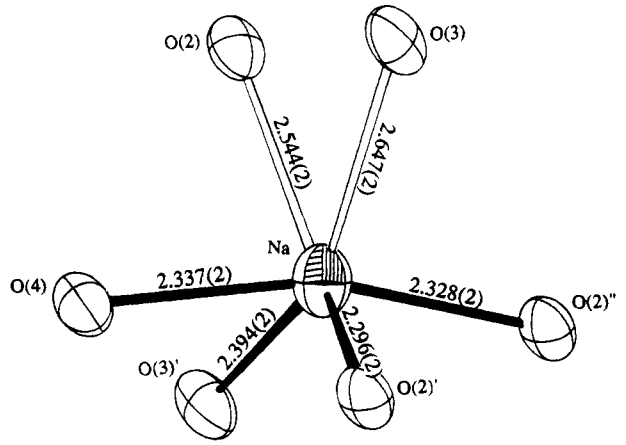

Figure 4. Distorted NaO_6 octahedral coordination geometry characterized by four short (solid lines) and two long (open lines) Na−O bonds. The anisotropic atoms are presented at 90% probability. The bond distances are in Å.

ribbons, and cap the space by forming three Na−O bonds. The other three Na−O bonds in the NaO_6 coordination are captured from the neighboring slab forming the three-dimensional lattice.

The irregular NaO_6 coordination may be viewed as having been derived from a largely distorted octahedron. In Figure 4, the NaO_6 coordination is viewed along the same direction as in Figure 2. The Na−O bond distances (Table 3), consist of four short (2.30−2.39 Å) and two long (2.54−2.65 Å) bonds, indicating that the sodium cation is off-centered with respect to the oxygen polyhedron. This distortion is presumably attributed to the neighboring sodium cations (3.09 Å) along the viewing direction in Figure 2. In any case, the averaged Na−O distance, 2.42 Å, is comparable to the sum of the Shannon crystal radii,[16] 2.38 Å, of the six-coordinated Na^+ (1.16 Å) and three-coordinated O^{2-} (1.40Å).

Table 3 also lists the important bond distances and angles that correspond to the geometry of the CuO_4 and the P_2O_7 polyhedra in the title compound. The distances and angles are comparable with those of the previously reported copper(II) phosphates. In comparison to the structurally closely related $Li_2CuP_2O_7$[6e] (see later discussion), the Cu−O bond distances are in the range of 1.91−1.96 Å for the title compound and 1.92−1.93 Å for the lithium analog, whereas the P−O bridging/terminal bond distances are 1.61 Å/1.49−1.53 Å vs 1.62 Å/1.48−1.53 Å, respectively. Although the PO_4 tetrahedron is distorted, its inhomogeneous bond distances can be qualitatively

(16) Shannon, R. D. *Acta Crystallogr.* **1976**, *A32*, 751.

Table 3. Important Bond Distances (Å) and Angles (deg) for $Na_2CuP_2O_7$

		CuO_4	
Cu−O(3)	1.962(2)	Cu−O(4)	1.911(2)
Cu−O(3)	1.962(2)	Cu−O(4)	1.911(2)
O(3)−Cu−O(3)	180.0	O(3)−Cu−O(4)	93.51(7)
O(3)−Cu−O(4)	86.49(7)	O(3)−Cu−O(4)	86.49(7)
O(3)−Cu−O(4)	93.51(7)	O(4)−Cu−O(4)	180.0
		2 PO_4 in P_2O_7	
P−O(1)	1.614(1)	P−O(3)	1.533(2)
P−O(2)	1.492(2)	P−O(4)	1.524(2)
O(1)−P−O(2)	107.7(1)	O(1)−P−O(3)	106.79(8)
O(1)−P−O(4)	105.93(8)	O(2)−P−O(3)	112.1(1)
O(2)−P−O(4)	112.8(1)	O(3)−P−O(4)	111.1(1)
P−O(1)−P	120.3(1)		
		NaO_6	
Na−O(2)	2.296(2)	Na−O(2)	2.544(2)
Na−O(2)	2.328(2)	Na−O(3)	2.647(2)
Na−O(3)	2.394(2)	Na−O(4)	2.337(2)
O(2)−Na−O(2)	141.87(7)	O(2)−Na−O(2)	89.60(6)
O(2)−Na−O(3)	91.32(7)	O(2)−Na−O(3)	117.89(8)
O(2)−Na−O(4)	88.89(7)	O(2)−Na−O(2)	111.84(7)
O(2)−Na−O(3)	57.74(6)	O(2)−Na−O(3)	91.65(7)
O(2)−Na−O(4)	79.95(7)	O(2)−Na−O(3)	93.07(7)
O(2)−Na−O(3)	96.33(7)	O(2)−Na−O(4)	161.43(7)
O(3)−Na−O(3)	149.25(6)	O(3)−Na−O(4)	105.47(7)
O(3)−Na−O(4)	68.23(7)		

Table 4. Observed and Calculated P−O distances[a,b] in $Na_2CuP_2O_7$

anion	ϱ_o	$\Delta\varrho_o$	d_{obs}, Å	d_{calc}, Å	$\lvert\Delta d\rvert$, Å
P−O(1)	2.50	0.48	1.614(1)	1.589	0.025
O(2)	1.75	−0.27	1.491(2)	1.508	0.016
O(3)	1.92	−0.10	1.533(2)	1.526	0.007
O(4)	1.92	−0.10	1.524(2)	1.526	0.002

[a] ϱ_o is the sum of the cation contributions for the bond interactions of a particular oxygen atom. $\Delta\varrho_o$ is the difference between ϱ_x ((number of positive charges)/CN) of one individual oxide and the mean ϱ_o of all oxides in the coordination polyhedron. d_{obs} is the observed P−O distance in the title compound. d_{calc} is the calculated bond distance from Baur's equation: $d_{calc} = 1.537 + 0.109\Delta\varrho_o$. Finally, $|\Delta d|$ is the difference between d_{obs} and d_{calc}. [b] The valence of each coordinated cation used in the above calculations are the following: Na^+, Cu^{2+}, P^{5+}. These cations contribute bond strengths, ϱ_x, of 0.17, 0.50, and 1.25, respectively.

justified by the electrostatic interaction that each oxygen in the P_2O_7 unit undergoes with the equation given by Baur.[17] The analysis procedures are the same as previously reported.[4] The resulting P−O bond distances (d_{calc}, Å) based upon the bond strengths that each cation contributes (Na^+, Cu^{2+}, P^{5+}) to the coordinated oxygen atoms are compared with the observed values (d_{obs}, Å) in Table 4. The results are generally satisfactory and complementary with the bond valence sum (BVS) analysis.[18] The results from the BVS calculations based upon observed bond distances are consistent with the assigned formal oxidation states of cations; the calculated phosphorus valence is +4.95 and the copper valence is +1.83. Thus, for the charge-balanced formula $Na_2CuP_2O_7$, the copper cation is assigned as divalent while sodium and phosphorus cations are monovalent and pentavalent, respectively.

The structure of $Na_2CuP_2O_7$ is closely related to that of its lithium analog, $Li_2CuP_2O_7$, and possibly that of the structurally unknown $K_2CuP_2O_7$ phase. Frameworks of both the lithium and sodium phases consist of the undulating $[CuP_2O_7]_\infty$ ribbon. The two unit cells, however, are different in their relative

(17) Baur, W. H. *Trans. Am. Crystallogr. Assoc.* **1970**, *6*, 129.
(18) Brown, I. D.; Altermatt, D. *Acta. Crystallogr.* **1985**, *B41*, 244.

orientation of $[CuP_2O_7]_\infty$ parallel ribbons. This variation is due to the different coordination geometries adopted by the corresponding A-site cations, LiO_4 vs NaO_6. An attempt to refine the present structure based on the atomic coordinates from the *I*2/a setting reported in the Li structure failed. The Cu−O−Cu and direct Cu−Cu bond interactions do not exist in either case, as might be expected because of the layered arrangement; the shortest Cu···Cu separation distance ($d_{Cu-Cu} \equiv c/2$) is 4.30 Å for the Li structure and 4.03 Å for the Na structure. The larger d_{Cu-Cu} observed in the Li structure is possibly the result of ribbon displacement to enhance the bonding to the Li cation which stretches the ribbon. It is also worth mentioning that the charge of the A-site cation is a determining factor in the formation of the three-dimensional framework. In $Sr_2CuSi_2O_7$, for example, the two structural units, CuO_4 and Si_2O_7, share one oxygen atom to accommodate the higher coordination number adopted by the Sr^{2+} cation and forms a channel structure instead of a layered one.

Although the cell constants of the above mentioned potassium analog have been indexed by the powder method in a tetragonal crystal system (a = 8.054 (4) Å, c = 10.970 (5) Å),[8] the single crystal structure is not yet known. Based upon the similarities of the IR spectra shown in Figure 1, the $K_2CuP_2O_7$ structure assuredly consists of P_2O_7 units, similar to those in the Li and Na structures. The connectivity of the CuO_4 and P_2O_7 units in the $K_2CuP_2O_7$ structure, however, may be different due to the distinct IR bands centered at much lower frequency, 705/908 cm^{-1}. The increased coordination number adopted by the large cation, K^+, may lead to the formation of an open framework structure where the CuO_4 unit shares each of its four corner oxygen atoms with a different P_2O_7 pyrophosphate. Nevertheless, the ion-exchange reaction results suggest a possible structural correlation in the $A_2CuP_2O_7$ family, in that the $K_2CuP_2O_7$ structure may consist of similar $[CuP_2O_7]_\infty$ chains. This proposed structure would require little bond rearrangement with regards to the connectivity between the CuO_4 and P_2O_7 units during the ion-exchange process. The crystal structure determination awaits the growth of single crystals.

In conclusion, the synthesis and crystal growth of a new sodium copper(II) pyrophosphate, $Na_2CuP_2O_7$, has been accomplished by employing a low-temperature eutectic halide flux. The structure is characterized by a layered framework, which is relatively rare among known copper-based phosphate and silicate compounds. Further analysis has shown that the extended $[CuP_2O_7]^{2-}$ slab structure is composed of unusual undulating $[CuP_2O_7]_\infty$ ribbons, which are recognized for the first time as being associated with the structures of the $A_2CuP_2O_7$ compound family. The adaptive bond interaction between CuO_4 and P_2O_7 units conceivably facilitates the formation of special frameworks.[19]

Acknowledgment. Financial support for this research (DMR-9208529) and the single crystal X-ray diffractometer from the National Science Foundation is gratefully acknowledged.

Supplementary Material Available: Tables of detailed crystallographic data and anisotropic thermal parameters (2 pages). Ordering information is given on any current masthead page.

IC9412466

(19) Etheredge, K. M. S.; Hwu, S.-J., *Inorg. Chem.*, submitted for publication.